Analyses of deuterium retention in tungsten and graphite first wall materials by laser-induced ablation spectroscopy on EAST

Jannis Oelmann[a], Zhenhua Hu[b,*], Cong Li[c], Liying Sun[c], Jiamin Liu[c], Fang Ding[b], Liang Wang[b], Sebastijan Brezinsek[a], Rui Ding[b], Hongbin Ding[c], Guangnan Luo[b], Junlin Chen[b], the EAST Team[b]

[a] *Forschungszentrum Jülich GmbH, Institut für Energie- und Klimaforschung – Plasmaphysik, Partner of the Trilateral Euregio Cluster (TEC), 52425 Jülich, Germany*

[b] *Institute of Plasma Physics, Chinese Academy of Sciences, Hefei, Anhui 230031, PR China*

[c] *Key Laboratory of Materials Modification by Laser, Ion and Electron Beams, Chinese Ministry of Education, School of Physics, Dalian University of Technology, 116024 Dalian, PR China*

Abstract

Plasma-wall interactions at the first wall in fusion experimental devices are critical for the life time of plasma-facing components and tokamak operation. In-situ measurements of these plasma-wall interaction processes are required in long pulse devices in order to understand better the underlying mechanisms as well as monitoring of the tritium content of the first wall as an immediate safety application. In this work we present measurements of the deuterium retention in the first wall of EAST using laser-induced ablation spectroscopy. The diagnostic is applied during plasma operation and the dynamic retention for graphite and tungsten as plasma-facing materials are compared, showing more than three times higher short-term retention in graphite than in tungsten. Laser-based analysis is applied during a shift of the vertical positions of the plasma column in limited as well as in the start-up phase of discharges in diverted magnetic configuration. Plasma core densities of $n_e = (1.5 - 3.2) \times 10^{19}/\mathrm{m}^3$ are chosen to vary the ion flux to the first wall and study saturation effects of deuterium on the surface first wall materials during tokamak plasma operation. A linear dependence of the retention from ion fluence is observed for graphite as PFC up to $3 \times 10^{18}\,\mathrm{D}^+/\mathrm{cm}^2$, followed by a constant retention up to fluences of $3.5 \times 10^{19}\,\mathrm{D}^+/\mathrm{cm}^2$ for nearby first wall temperatures of $T_{\mathrm{PFC}} \approx 350\,\mathrm{K}$.

Keywords: Laser–induced ablation spectroscopy, Plasma-facing components, Deuterium retention, In-situ analysis, EAST tokamak

Highlights

- Combined LIBS and LIAS measurements were applied to determine the dynamic deuterium retention in C and W during EAST discharges.
- LIAS measurements show more than three times higher deuterium retention in graphite than in tungsten during EAST discharges.
- The deuterium retention on the graphite PFC is saturated within 0.2 s plasma exposure for limited magnetic configuration when the plasma actively touches the first wall.
- The deuterium retention in the start-up phase is significantly larger than during the discharge for diverted magnetic configuration.

1. Introduction

To demonstrate the capability of quantitative deuterium retention determination of Plasma-Facing Components (PFCs) by laser-based techniques during discharges is a key challenge in fusion research. It is investigated as candidate for in-vessel fuel retention determination in long pulse devices with actively cooled PFCs [1, 2] and can help to increase the understanding of Plasma-Wall Interactions (PWI) like material deposition and transport [3, 4]. Laser-Induced Breakdown Spectroscopy (LIBS) [5, 6] results show that this technique is suitable for measurements of hydrogen isotope retention in materials like C and W [7, 8].

Laser-Induced Ablation Spectroscopy (LIAS) is an operando method for fuel retention analysis [9, 10, 11] in which a short, intensive laser pulse ablates first wall material during the discharges. Atoms of the ablated surface layer enter the edge plasma of the tokamak, are excited and emit characteristic radiation with higher emission intensities than for LIBS [12], which consequently can increase the limit of detection.

The Experimental Advanced Superconducting Tokamak (EAST) is very suitable for PWI investigations with its capabilities of long-pulse and high-performance operation, like a stable steady-state high confinement plasma of more than 100 s [13]. Thus the deuterium recycling and wall re-

*Corresponding author.
Email address: huzh@ipp.ac.cn (Zhenhua Hu)

tention can be determined multiple times during one discharge for which the combined LIBS and LIAS measurement technique was demonstrated successfully in EAST before [14]. In this publication results are presented in which LIAS measurements were performed during programmed vertical movements of the plasma column which vary the incident ion flux to the first wall at the measurement location on the High Field Side (HFS) of the tokamak. Optical emission of Balmer lines during the LIAS process are compared with ion flux measurements carried out with nearby located Langmuir probes. The analysis is applied for discharges of different densities in limited magnetic configuration of EAST with ion fluxes of several A/cm^2 to the first wall to check the influence and fuel retention behavior in the start-up phase of discharges in diverted magnetic configuration.

2. Experimental Setup

The combined LIAS and LIBS setup for in-situ and possible operando short-term deuterium retention analysis of different first wall materials is located at the H-port of EAST. In this section an overview of the main aspects of the setup is given, a more detailed description can be found in previous publications [14, 15].

2.1. Setup for laser-induced analysis of the first wall

The output of a short, intensive pulse Nd:YAG laser is guided via a focusing optical lens and through a quartz glass window into the main vacuum vessel of EAST and onto the first wall HFS. With a laser wavelength of $\lambda_p = 1064\,\mathrm{nm}$, a pulse duration of $t_p = 6\,\mathrm{ns}$ and pulse energies of $E_p = 200\,\mathrm{mJ}$, several tens of nanometers of the first wall material are ablated locally whereas the rate depends on the investigated material itself. For the deuterium retention analysis, samples of molybdenum (Mo), Doped graphite (C: *GBST1308* 1%B_4C, 2.5%Si, 7.5%Ti with thick SiC gradient coatings [16]) and tungsten (W) with a size of $1\,\mathrm{cm}^2$ each are embedded in the first wall tiles, which can be seen in a camera picture in Fig. 1. The analyzed PFCs are located below the mid-plane of the tokamak and thus below the central position of the plasma column in limited configuration. The laser pulses induce crater with a diameter of $d_{\mathrm{Cr}} \approx 1.5\,\mathrm{mm}$ in the ablation process [14].

A second window, adjacent to the one for laser excitation is used for observation of the laser-induced radiation at the first wall materials surface (LIBS) and of the ablated atoms entering the edge plasma of the tokamak (LIAS). A beam splitter divides the emitted radiation into two light paths with equivalent intensities. One path of the radiation is analyzed by a high speed camera for LIAS analysis, which is presented in the following section. The second part uses a collection lens to guide the emitted radiation to an optical fiber which is connected to a spectrometer for LIBS analysis. Here characteristic line emissions depict the wall material, retained fuel as well as impurities.

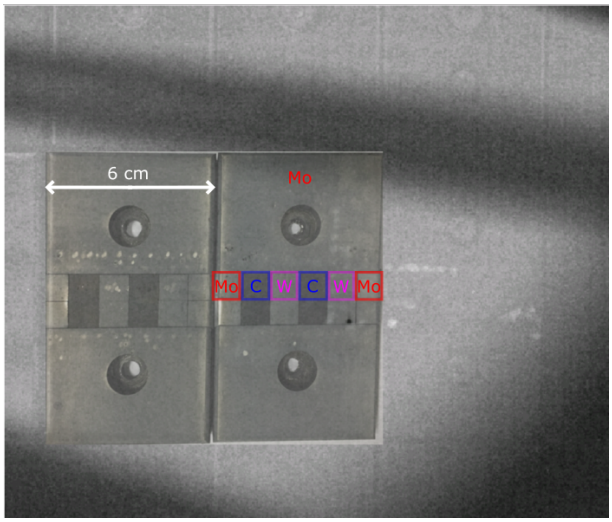

Fig. 1. Camera image of the HFS at H-port with Mo, C and W samples on the Mo first wall. A photo of two dismounted first wall tiles with the sample inlets is overlayed.

LIBS measurements [17, 18] are performed simultaneously to LIAS, but will not be discussed in this publication. Within the experiments, LIBS signals are used to confirm the analyzed first wall material which is ablated by the laser pulses.

2.2. LIAS signal analysis

When the laser-induced ablated atoms enter the edge plasma, again characteristic radiation is emitted. The high speed camera (*PCO dimax S* with 1102 fps and CMOS image sensor *S4*: 2016 × 2016 pixel, 11 μm × 11 μm pixel size) for deuterium retention analysis is equipped with a narrowband filter (central wavelength = 656.3 nm, bandwidth $I_{50\%} = 1.5\,\mathrm{nm}$) to detect D_α radiation spatially- and time-resolved. A long time exposure image with $\Delta t_{\mathrm{i}} = 1.5\,\mathrm{s}$ is shown in Fig. 1 to visualize the analyzed field of view. Three entire inner wall Mo tiles are observed in the center of the frame with covered sections in the upper part by a bar and the lower corners. The shadowed parts only slightly influence the data evaluation as they are not close to the the analyzed first wall material samples. A photo of two dismounted first wall tiles with Mo, C and W samples in the center is overlayed in Fig. 1. Light dots on the sample show laser-induced craters in the first wall materials.

For the deuterium retention studies during the EAST discharges, an exposure time of $\Delta t_{\mathrm{i}} = 100\,\mu\mathrm{s}$ is chosen to integrate over the whole radiation emission caused by one laser-induced ablation. With an almost collinear arrangement of laser excitation and observation angle, also the emission of radiation at the surface of the PFC (which is also analyzed by LIBS) is detected with the camera. Camera images of laser-induced interactions at time t_{LP} with the EAST discharge starting at $t = 0\,\mathrm{s}$ are shown in Fig. 2. The toroidal and poloidal coordinates x and y

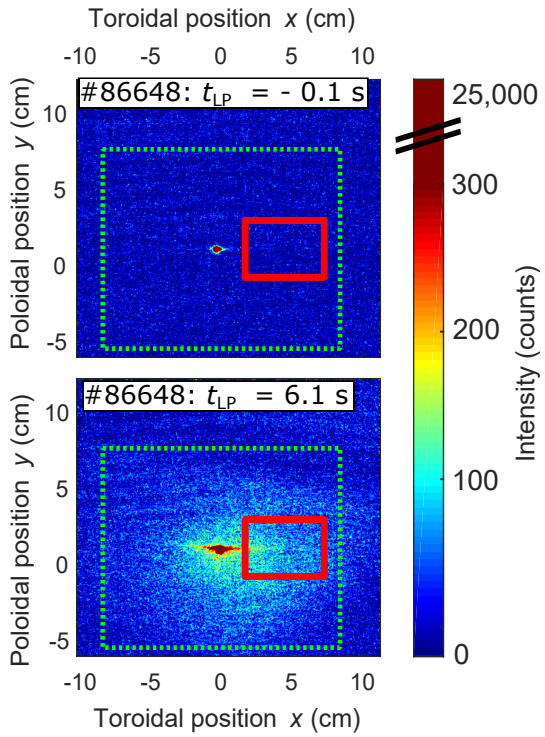

Fig. 2. Camera image ($\Delta t_i = 100\,\mu$s) of D_α radiation after laser-induced ablation of graphite PFC before (top) and during (bottom) EAST discharge #66648. The evaluated regions of interest for LIAS analyses are shown as red and green boxes.

refer to the dimensions at the HFS first wall and are determined from Fig.1 with known sample sizes. The first image at $t_{LP} = -0.1$ s shows the laser-induced interaction at the surface of the first wall without EAST plasma (in following called *LIBS signal*). The position $x/y = 0\,\text{mm}/0\,\text{mm}$ is set as the laser-induced interaction position with the PFC. The diameter (full-width at half maximum in toroidal direction) of the emission plume is 0.5 cm. In addition to the LIBS signal, the second image shows the emission of ablated deuterium atoms entering the edge plasma with a plume diameter (D_α emission greater than the noise level) of more than 10 cm. The integrated signal from the green box shown in Fig. 2, including the LIBS signal, is used for a comparison of the retention in graphite and tungsten. To exclude the LIBS signal, alternatively the integrated camera signal from the red boxes is taken for the LIAS analysis, which is called *LIAS intensity* in following sections. For each image and for the *LIAS intensities* the average signal of two camera images taken 218 μs and 109 μs earlier is subtracted to exclude the time depended D_α radiation from the EAST plasma. Average signals of the boxes are compared in section 4, Table 1.

3. EAST discharge parameters

The presented analyses were performed for deuterium discharges. Dedicated experiments with a variation of the vertical plasma column for discharges in limited magnetic

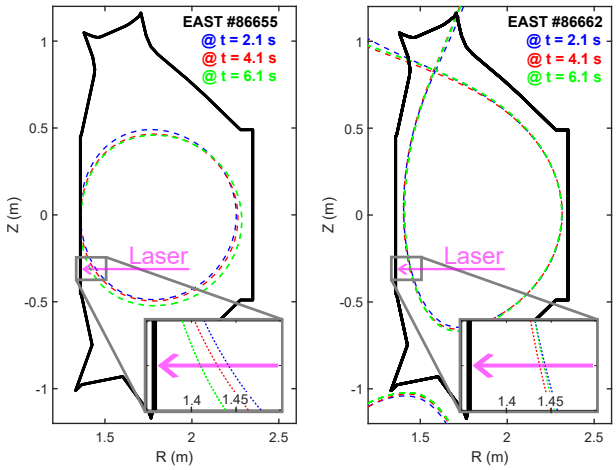

Fig. 3. Magnetic reconstruction of the LCFS for limited and diverted magnetic configuration. The colors indicated different times where LIAS is applied: $t = 2.1$ s, $t = 4.1$ s and $t = 6.1$ s.

configuration as well as studies of the start-up phase in diverted magnetic configuration are evaluated.

A limited magnetic configuration was chosen to have significant particle flux to the first wall PFCs during the discharges optimized to apply LIBS and LIAS on first wall samples. The plasma is shifted downwards within the flat top phase of the discharge. A magnetic reconstruction of the LCFS for several times where LIAS is applied is shown together with the sample location in Fig. 3. As shown in Fig. 4, a shift by 4.5 cm is achieved which results in variation of the ion flux to the limiter due to larger distance between the Last Closed magnetic Flux Surface (LCFS) and the measurement location at the limiter. Three dedicated discharges are shown to demonstrate the equivalent column shifting for different plasma densities. The ion flux Γ to the wall on the HFS in H section of the tokamak is determined from saturation current measurements by a triple langmuir probe nearby the samples for laser-induced analyses. As the vertical position of the plasma column is shifted only by a few centimeters, only a moderate increase of Γ is observed during the movement. As the analyzed PFCs are located below the mid-plane, the spacial distribution of the ablated particles entering the plasma varies for different position of the LCFS. Still, the observed volume is large enough to detect the LIAS signal for the different plasma columns. The times of the laser-induced PFC analyses are marked in blue in Fig. 4. Five laser pulses are used before the discharge to clean the surface of the analyzed PFC position from lithium and establish equivalent conditions. Two laser pulse are applied after the start-up phase and four laser pulses during the shifting of the vertical plasma column. The exposure time of the PFC in between the laser-based analysis is $\Delta t_{exp} = 0.2$ s to $\Delta t_{exp} = 2.1$ s. Measurements of the infrared thermographic system nearby the location for laser-induced PFC analyses show a slight increase of the first wall temperatures from $T_{PFC} = 338$ K to $T_{PFC} = 342$ K.

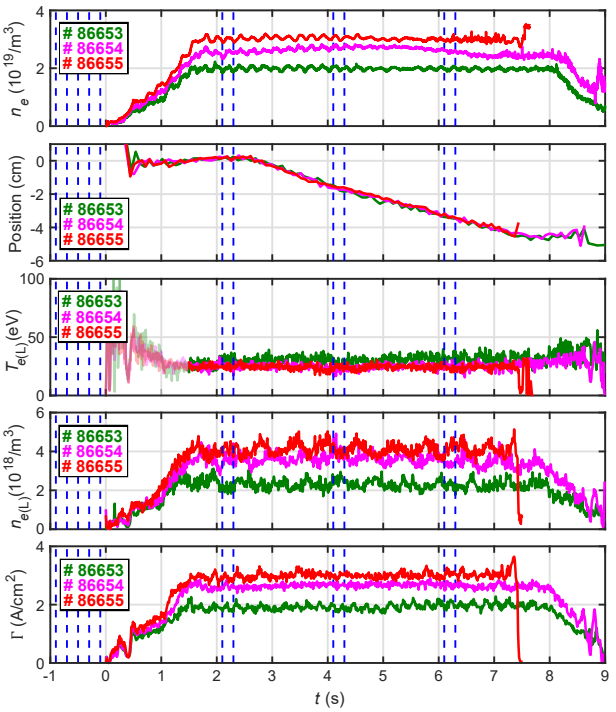

Fig. 4. Electron density n_e and the vertical position of the plasma column in limited magnetic configuration discharges with HFS triple langmuir probe measurements of the electron density $n_{e(\mathrm{L})}$, temperature $T_{e(\mathrm{L})}$ and ion flux to first wall Γ. The times of the laser-induced analyses are shown in blue.

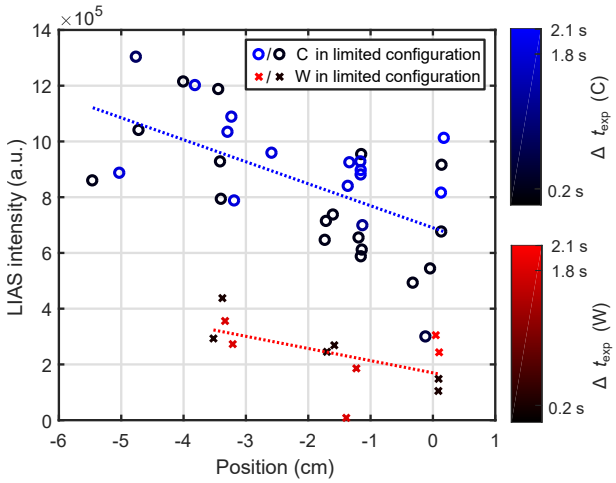

Fig. 5. LIAS deuterium signal over the vertical position of the plasma column in limited configuration. The exposure time of the analyzed PFC location t_{exp} is shown color coded for C in blue circles and W in red crosses.

Table 1: Average high speed camera signal counts of the LIAS deuterium intensities I in Fig. 5 for box 1 and box 2 shown in Fig. 2.

PFC	C		W		C/W
Emission in	LIBS	LIAS+LIBS	LIBS	LIAS+LIBS	LIAS ratio
		in 10^5 counts			
I(box 1)	-	8.43	-	2.39	3.5
I(box 2)	3.56	56.46	1.63	17.42	3.4

In the measurements with diverted magnetic configuration, which is present after the start-up phase of $t \leq 0.9$ s, the laser-induced analysis is performed every $\Delta t_{\mathrm{exp}} = 0.2\,\mathrm{s}$ during the start-up phase.

4. Results and discussion

4.1. Plasma column variation

For discharges in limited magnetic configuration, LIAS intensities (counts added up from the red box in Fig. 2) are shown in Fig. 5 over the vertical position of the plasma column. The LIAS intensity is rising as the plasma is shifted downwards, both for an analysis of the deuterium retention in C (blue circles) and in W (red crosses). Linear fit lines are shown as guide to the eye. The average deuterium signal for laser-induced ablation of W as PFC is 3.5 times lower than for C. Moreover Fig. 5 shows that only a moderate dependence on the exposure time Δt_{exp} of the PFCs, shown as color of the data points, is observed. This will be further discussed in section 4.2.

To compare the deuterium retention in graphite and tungsten, the whole LIAS signal needs to be evaluated. The average deuterium intensities for two regions of interest, shown as boxes in Fig. 2, can be found in Table 1.

For box 2, the average camera picture intensity of a laser-induced ablation without EAST plasma operation is subtracted to calculate the LIAS signal without LIBS signal. The laser-induced emission at the first wall surface is not included in the signal of box 1.

In C a 3.4 times higher LIAS intensities signal is observed than in W. This ratio of LIAS intensities is equal to the ratio of the deuterium retention in graphite and tungsten if a perturbation of the EAST plasma by the ablated atoms is neglected and edge plasma parameters are equivalent for analysis of C and W as PFC. Note that the thermal penetration depth of the laser is higher in W and thus more desorbed deuterium from the surrounding material is released than for C. Consequently the ratio of 3.4 is a lower limit of the deuterium retention C to W ratio. Also a possible influence from lithium on the surface of surrounding material is neglected.

4.2. D retention dependence on the ion fluence

The low dependence of the LIAS intensity on the exposure time Δt_{exp} and thus the ion fluence indicates, that the deuterium retention can be saturated already after 0.2 s of plasma operation in flat top phase for limited magnetic configuration with the present plasma densities. In Fig. 6 the LIAS intensity of graphite as PFC is plotted over the ion fluence to the first wall, determined by langmuir probe measurements of the ion flux times the exposure time Δt_{exp} of the PFCs. For fluences $F \geq 3 \times 10^{18}\,\mathrm{D^+/cm^2}$

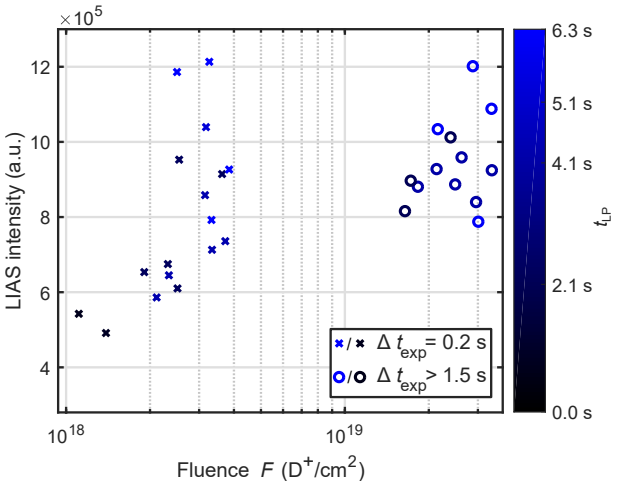

Fig. 6. Deuterium signal over ion fluence measured by a langmuir probe for an analysis of graphite as PFC. The time of the laser pulse t_{LP} color coded and different exposure times Δt_{exp} are shown with different markers.

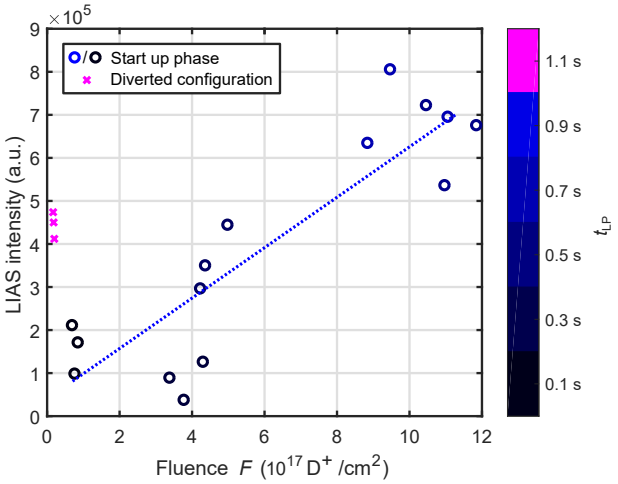

Fig. 7. LIAS intensity of deuterium in graphite for the start-up phase (circles) and in diverted magnetic configuration (crosses) for discharges #93922 to #93924. The time of the laser pulse is shown color coded.

the LIAS intensities are as high for $\Delta t_{\mathrm{exp}} = 0.2\,\mathrm{s}$ as for $\Delta t_{\mathrm{exp}} > 1.5\,\mathrm{s}$ within the signal fluctuation. Consequently here a near-surface saturation is reached for the present EAST plasma properties and a local equilibrium of D retention is present. For $F < 3 \times 10^{18}\,\mathrm{D^+/cm^2}$ LIAS intensities are lower for minor fluences.

4.3. Start up phase analysis

To analyze a lower respectively ion fluence or flux regime, the start-up phase of EAST discharges in diverted magnetic configuration is investigated. Fig .7 shows the LIAS intensities over the fluence of three discharges. For these measurements, the beam splitter in the collection optics of the LIAS set up was replaced by an optical mirror to analyze the whole signal with the high speed camera. The LIAS intensity signals in Fig .7 were reduced by 50% to have equivalent intensities like in the previous data of Fig. 6.

Within the start-up phase, a linear rise of the deuterium signal is observed. When the diverted configuration is reached after $t = 0.9\,\mathrm{s}$ and the ion flux is much lower, the deuterium retention is reduced by about 35% (pink crosses). The LIAS intensities for fluences of $F \approx 1 \times 10^{18}\,\mathrm{D^+/cm^2}$ during the start-up phase are in good agreement with equivalent fluences observed in limited configuration in Fig. 6. Note that here the edge plasma conditions are not as stable as in the flat top phase of the dedicated discharges in limited configuration. Still, the LIAS intensities for $F = 1 \times 10^{18}\,\mathrm{D^+/cm^2}$ in start-up phase are significantly larger than during diverted magnetic configuration.

5. Conclusion and outlook

LIAS and LIBS diagnostic were applied simultaneously on first wall materials tungsten and graphite to monitor the dynamic deuterium content during EAST operation. The short-term deuterium retention on graphite surface was found to be over 3.4 times higher than for tungsten for ion fluxes of $\Gamma = (2-3)\,\mathrm{A/cm^2}$ and first wall temperatures of $T_{\mathrm{PFC}} \approx 350\,\mathrm{K}$. A saturation effect of the deuterium retention on graphite as plasma-facing component on the first wall high field side was determined for ion fluences of $F \geq 3 \times 10^{18}\,\mathrm{D^+/cm^2}$. For the start-up phase of discharges in diverted magnetic configuration, a linear dependence of the deuterium retention to ion fluences in a range of $F \approx \left(10^{17} - 10^{18}\right)\mathrm{D^+/cm^2}$ was found for graphite first wall PFCs.

In future studies the combined LIBS and LIAS setup will be used at EAST to determine the fluence dependence of deuterium retention also for tungsten as first wall PFC. Moreover the helium interaction with tungsten first wall components and retention for helium discharges will be investigated.

Acknowledgment

This work has been carried out within the framework of the EUROfusion Consortium and has received funding from the Euratom research and training programme 2014-2018 and 2019-2020 under grant agreement No 633053. The views and opinions expressed herein do not necessarily reflect those of the European Commission.

This work was supported within the SINO-GERMAN project by the Deutsche Forschungsgemeinschaft and the National Nature Science Foundation of China under Contract No11861131010.

References

[1] M. Zlobinski, V. Philipps, et al., Laser induced desorption as tritium retention diagnostic method in ITER, Fusion Eng. Des. 86 (6-8) (2011) 1332–1335. doi:10.1016/j.fusengdes.2011.02.030.

[2] A. Bultel, V. Morel, et al., Towards ps-LIBS tritium measurements in W/Al materials, Fusion Eng. Des. 146 (April) (2019) 1971–1974. doi:10.1016/j.fusengdes.2019.03.079.

[3] R. Hai, P. Liu, et al., Collinear double-pulse laser-induced breakdown spectroscopy as an in-situ diagnostic tool for wall composition in fusion devices, Fusion Eng. Des. 89 (9-10) (2014) 2435–2439. doi:10.1016/j.fusengdes.2014.04.065.

[4] S. Brezinsek, J. Coenen, et al., Plasma–wall interaction studies within the EUROfusion consortium: progress on plasma-facing components development and qualification, Nucl. Fusion 57 (11) (2017) 116041. doi:10.1088/1741-4326/aa796e.

[5] C. Li, C. L. Feng, et al., Review of LIBS application in nuclear fusion technology, Front. Phys. 11 (6). doi:10.1007/s11467-016-0606-1.

[6] S. Carter, R. Clough, et al., Atomic spectrometry update: review of advances in the analysis of metals, chemicals and materials, J. Anal. At. Spectrom. 30 (11) (2019) 2249–2294. doi:10.1039/C9JA90058F.

[7] A. Semerok, D. L'Hermite, et al., Laser induced breakdown spectroscopy application in joint European torus, Spectrochim. Acta - Part B At. Spectrosc. 123 (2016) 121–128. doi:10.1016/j.sab.2016.08.007.

[8] D. Zhao, C. Li, et al., Temporal and spatial dynamics of optical emission from laser ablation of the first wall materials of fusion device, Plasma Sci. Technol. 20 (1). doi:10.1088/2058-6272/aa96a0.

[9] A. Huber, B. Schweer, et al., Development of laser-based diagnostics for surface characterisation of wall components in fusion devices, Fusion Eng. Des. 86 (6-8) (2011) 1336–1340. doi:10.1016/j.fusengdes.2011.01.090.

[10] M. Tokar, N. Gierse, et al., Modeling of plasma distortions by laser-induced ablation spectroscopy (LIAS) and implications for the interpretation of LIAS measurements, Nucl. Fusion 55 (11) (2015) 113017. doi:10.1088/0029-5515/55/11/113017.

[11] N. Gierse, M. Z. Tokar, et al., Time resolved imaging of laser induced ablation spectroscopy (LIAS) in TEXTOR and comparison with modeling, Phys. Scr. T167 (2016) 014034. doi:10.1088/0031-8949/T167/1/014034.

[12] V. Philipps, A. Malaquias, et al., Development of laser-based techniques for in situ characterization of the first wall in ITER and future fusion devices, Nucl. Fusion 53 (9) (2013) 93002. doi:10.1088/0029-5515/53/9/093002.

[13] L. Wang, H. Y. Guo, et al., Advances in plasma-wall interaction control for H-mode operation over 100 s with ITER-like tungsten divertor on EAST, Nucl. Fusion 59 (8). doi:10.1088/1741-4326/ab1ed4.

[14] Z. Hu, N. Gierse, et al., Development of laser-based technology for the routine first wall diagnostic on the tokamak EAST : LIBS and LIAS, Phys. Scr. T170 (2017) 014046. doi:10.1088/1402-4896/aa8650.

[15] Z. Hu, N. Gierse, et al., Laser induced ablation spectroscopy for in situ characterization of the first wall on EAST tokamak, Fusion Eng. Des. 135 (July) (2018) 95–101. doi:10.1016/j.fusengdes.2018.07.017.

[16] C. Xie, J. Chen, et al., Surface modification of thick SiC gradient coatings on doped graphite under long pulse plasma irradiation, J. Nucl. Mater. 363-365 (2007) 282–286. doi:10.1016/j.jnucmat.2007.01.193.

[17] Z. Hu, C. Li, et al., Preliminary results of in situ laser-induced breakdown spectroscopy for the first wall diagnostics on EAST, Plasma Sci. Technol. 19 (2). doi:10.1088/2058-6272/19/2/025502.

[18] D. Zhao, C. Li, et al., Remote in situ laser-induced breakdown spectroscopic approach for diagnosis of the plasma facing components on experimental advanced superconducting tokamak, Rev. Sci. Instrum. 89 (7). doi:10.1063/1.5024848.